

# Polymerization Kinetics and Monomer Functionality Effects in Thiol–Ene Polymer Dispersed Liquid Crystals

Timothy J. White,<sup>†</sup> Lalgudi V. Natarajan,<sup>‡</sup> Vincent P. Tondiglia,<sup>‡</sup>  
Timothy J. Bunning,<sup>§</sup> and C. Allan Guymon<sup>\*,†</sup>

Department of Chemical and Biochemical Engineering, The University of Iowa, Iowa City, Iowa 52245; Science Applications International Corporation, 3031 Colonel Glenn Highway, Dayton, Ohio 45431; and Materials and Manufacturing Directorate, Air Force Research Laboratory, Wright-Patterson AFB, Ohio 45433

Received August 10, 2006; Revised Manuscript Received December 1, 2006

**ABSTRACT:** Polymer dispersed liquid crystals (PDLCs) are a class of electrooptic materials most often formed by polymer-induced phase separation, a one-step fabrication technique often based on photopolymerization of the commercial thiol–ene mixture NOA65. To allow further understanding regarding PDLC formation, this work systematically examines processing variables that influence thiol–ene-based PDLC morphology and subsequent performance, namely polymerization kinetics, polymer gel point, and liquid crystal (LC) phase separation. PDLC formulations containing a wide range of thiol and ene monomers were examined as a function of monomer (thiol and ene) functionality, thiol–ene stoichiometry, and ene monomer composition. Simultaneous examination of polymer evolution and LC phase separation by real-time infrared (RTIR) spectroscopy shows that both polymerization kinetics and the gel point of thiol–ene PDLC formulations are influential on the extent of LC phase separation. Increasing monomer functionality (both thiol and ene) reduces LC droplet size in PDLC morphology by reducing the gel point conversion of thiol–ene polymer. In addition to influencing gelation, increasing the functionality or the electron density of ene monomer increases the rate of polymerization which further reduces LC droplet size. The thiol–ene PDLC formulations studied exhibit decreased LC droplet size (from 1  $\mu\text{m}$  to 300 nm) that correlates directly to polymerization rate and gel point. Electrooptic switching behavior is also dependent on LC droplet size.

## Introduction

Polymer dispersed liquid crystals (PDLCs) are a polymer/liquid crystal (LC) composite material proposed for applications in switchable windows and imaging technology<sup>1–3</sup> due to their unique electrooptic performance characteristics. Since the original report of these materials,<sup>4</sup> researchers have extensively examined PDLC formation seeking optimized performance. Much of this work has focused on correlating PDLC morphology to performance parameters such as on-state transmission, off-state scattering, and switching voltage.<sup>5–7</sup>

PDLCs are often formed through polymer-induced phase separation,<sup>8–10</sup> a one-step fabrication technique, in which a polymerization initially occurs in an isotropic mixture of LC and monomer. The formation of PDLCs is typically induced by photopolymerization (UV-curing).<sup>11</sup> With polymerization, the LC loses solubility in the polymer and separates into a distinct phase through either liquid–liquid or liquid–gel demixing. Upon phase separation, PDLCs take one of two morphologies: droplet (“Swiss cheese”) or interconnected (polymer ball). PDLCs form droplet or interconnected morphology based on LC concentration, polymerization mechanism, polymerization kinetics, and polymer composition.<sup>2</sup>

A number of studies examining PDLCs have utilized the commercial thiol–ene mixture NOA65 (Norland Products),<sup>12–18</sup> reportedly a mixture of trifunctional thiol (trithiol) and a tetrafunctional urethane allyl ether.<sup>19</sup> In addition to formation

using thiol–ene polymer systems, PDLCs have been fabricated using acrylates<sup>20–22</sup> and epoxides.<sup>23–25</sup> The polymer composition of the PDLC is critical in influencing performance characteristics such as switching voltage and transmittance. For example, incorporating fluorinated acrylates into PDLCs reduces LC anchoring energy and subsequently lowers switching voltage.<sup>26</sup>

Despite significant use of thiol–ene polymers as hosts for LC composites, until recently, the fundamentals of thiol–ene polymerizations have not been widely studied. Recent interest in thiol–ene photopolymerization has been motivated by the resilience of thiol–ene polymerization to oxygen inhibition and a wide array of thermomechanical properties,<sup>27</sup> thus making thiol–ene polymers attractive for standard UV-curing applications such as coatings. The kinetics of thiol–ene polymerization have long been known to be dependent on the electron density of the ene monomer and the chemical composition of the thiol monomer (i.e., aliphatic or mercaptopropionate thiol).<sup>28</sup> The numerous commercially available thiol and ene monomers of various functionality can change polymerization kinetics and allow the gel point of these polymers to be varied from conversions as low as 33% to as late as 71% in stoichiometrically balanced cross-linked systems.<sup>29,30</sup> Research regarding thiol–ene photopolymerization has been thoroughly reviewed by Hoyle<sup>31</sup> and also Jacobine.<sup>32</sup>

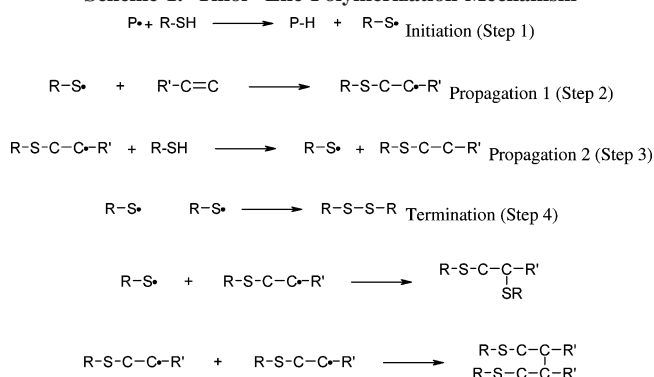
Thiol–ene polymerization occurs via a free radical step-growth mechanism. As shown in Scheme 1, the first step in thiol–ene polymerization is formation of initiating radical species through the absorption of light. In thiol–ene polymerization, these radical species subsequently abstract a hydrogen atom from thiol monomer to generate a thiyl radical (step 1, Scheme 1). Since thiyl radicals do not polymerize with other thiol monomer, the only means by which this radical can

\* To whom correspondence should be addressed: Tel (319) 335-5015, Fax (319) 335-1215, e-mail allan-guymon@uiowa.edu.

<sup>†</sup> The University of Iowa.

<sup>‡</sup> Science Applications International Corporation.

<sup>§</sup> Air Force Research Laboratory.

**Scheme 1. Thiol–Ene Polymerization Mechanism**

propagate is through addition across a carbon–carbon double bond (“ene” monomer). As shown in step 2 of Scheme 1, the addition of the thiyl radical across the ene monomer results in generation of a carbon-based radical species. In traditional thiol–ene polymerizations, ene monomers are chosen that do not readily homopolymerize. However, as shown in step 3 of Scheme 1, these carbon-based radical species will readily abstract a hydrogen atom from thiol monomer to regenerate a thiyl radical species. Thiol–ene polymerization continues through alternation of steps 2 and 3 of Scheme 1 until the radical species terminate, as shown in step 4.

The benefits of thiol–ene polymer in LC systems have been demonstrated recently in holographic polymer dispersed liquid crystals (HPDLCs).<sup>33</sup> Switching from the standard acrylate-based HPDLC formulation to a thiol–ene formulation based in NOA65 has resulted in dramatic performance enhancement. HPDLCs made from thiol–ene polymer show improved diffraction efficiency and greater LC droplet uniformity and do not suffer from the long-term degradation reported in acrylate-based materials. The performance enhancement of HPDLCs based on the commercial thiol–ene mixture NOA65 has motivated additional study into new thiol–ene formulations as an approach to further optimize HPDLC performance.<sup>34</sup>

While a great deal of research has studied thiol–ene-based PDLCs, these examinations have been nearly exclusively limited to NOA65. Correlating the influence of compositional changes in thiol–ene PDLC formulations to polymerization kinetics, LC phase separation and polymer/LC morphology may lead to more comprehensive understanding of PDLC formation and electrooptic properties, useful not only for optimizing PDLC performance but also laying a foundation for understanding the critical factors governing the fabrication of thiol–ene-based HPDLCs. In this paper, the formation of PDLCs is studied as a function of thiol and ene monomer functionality, thiol–ene stoichiometry, and ene monomer electron density. The kinetics of PDLC polymerization are studied simultaneously with direct examination of LC phase separation by real-time infrared spectroscopy (RTIR). The understanding gained through RTIR examination of polymerization kinetics and LC phase separation is complemented by scanning electron microscopy (SEM) imaging of PDLC morphology. Ultimately, the influence of monomer functionality on electrooptic switching behavior of fabricated PDLCs is determined and compared to NOA65-based PDLCs.

**Experimental Section**

**Materials.** All PDLC formulations examined contain 1 wt % Darocur 4265 (DC-4265, Ciba) and 30 wt % BL037 (EMD Chemical), a mixture of cyanobiphenyl liquid crystals. DC-4265 is a 50:50 weight mixture of 2-hydroxy-2-methyl-1-phenyl-1-

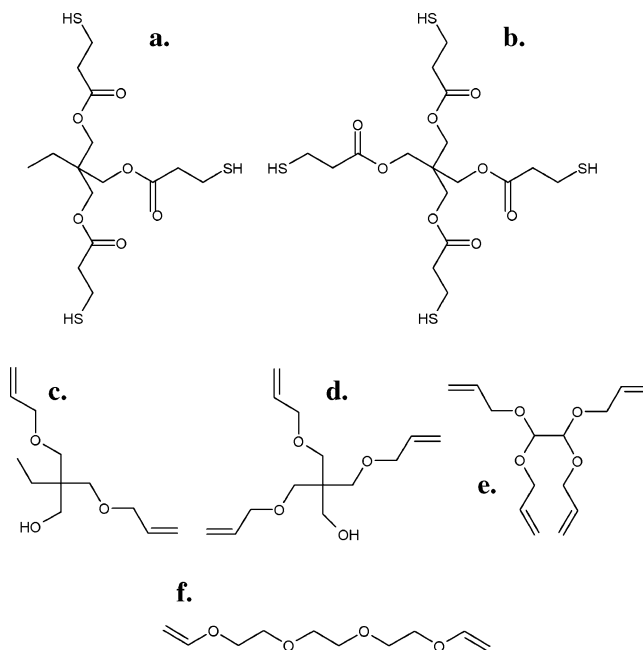


**Figure 1.** Chemical structures of thiol and ene monomers used in this study: (a) trithiol, (b) tetrathiol, (c) diene, (d) triene, (e) tetraene, and (f) divinyl ether.

**Table 1. Calculated Gel Points for PDLC Formulations**

name	molar ratio (thiol to ene)	stoichiometric ratio (thiol to ene)	calcd gel point (%)
trithiol/diene	1:1.5	1:1	71
1:0.66 trithiol/diene	1:1	1:0.66	86
1:1.33 trithiol/diene	1:2	1:1.33	81
tetrathiol/tetraene	1:1	1:1	33
trithiol/triene	1:1	1:1	50
trithiol/tetraene	1.33:1	1:1	41
trithiol/divinyl ether	1:1.5	1:1	71

propanone (Darocur 1173) and diphenyl (2,4,6-trimethylbenzoyl)phosphine oxide (Darocur TPO). Most PDLC formulations in this report contain the trifunctional thiol monomer trimethylolpropane tris(3-mercaptopropionate) (trithiol, Aldrich) and the difunctional ene monomer trimethylolpropane diallyl ether (diene, Aldrich). The influence of thiol and ene monomer functionality was investigated by comparing the trithiol/diene formulation to other mixtures including the tetrafunctional thiol monomer pentaerythritol tetrakis(3-mercaptopropionate) (tetrathiol, Aldrich), the trifunctional ene monomer pentaerythritol allyl ether (triene, Aldrich), or the tetrafunctional ene monomer glyoxal bis(diallyl acetal) (tetraene, Aldrich). PDLCs made from these allyl ether monomers were also compared to the difunctional ene monomer triethylene glycol divinyl ether (divinyl ether, Aldrich). Thiol–ene-based PDLCs were also compared to an acrylate-based PDLC formulation previously reported.<sup>35</sup> The acrylate-based formulation contains the highly functional monomer dipentaerythritol pentaacrylate (DPPA, Aldrich) mixed with 10 wt % *N*-vinyl pyrrolidone (NVP, Aldrich), 5 wt % octanoic acid (Aldrich), and 30 wt % BL037. All materials were used as received. Chemical structures for trithiol, tetrathiol, diene, triene, tetraene, and divinyl ether are shown in Figure 1.

**Thiol–Ene PDLC Formulations.** Unless otherwise noted, thiol and ene monomer were stoichiometrically balanced; i.e., equal numbers of both thiol and ene functional groups were used to allow optimal conversion of monomer in the PDLC mixtures. The compositions of the PDLC formulations studied here are listed in Table 1. The gel point for the thiol–ene polymers range from 33 to 86%, as calculated with the well-known gel point equation.<sup>36</sup> The stoichiometrically balanced (1:1) trithiol/diene PDLC formulation was compared to samples with excess ene (1:1.33 thiol to ene) and excess thiol (1:0.66 thiol to ene). Influencing the reaction stoichiometry in polymerization of two or more monomers is known

to shift the theoretical gel point to higher monomer conversion.<sup>36</sup>

**Methods.** A Fourier transform infrared (FTIR) spectrometer (Thermo Electron Nexus 670) with a liquid nitrogen cooled MCT detector was adapted to enable real-time study of photopolymerization (RTIR). The RTIR was purged with nitrogen to reduce noise from water vapor and carbon dioxide. A horizontal transmission accessory<sup>37</sup> fitted to the FTIR allows examination of photopolymerization in a nitrogen-rich environment free of oxygen. Samples containing 15  $\mu\text{m}$  glass spacers were sandwiched between two NaCl slides (International Crystal Labs). Photopolymerization was initiated by a high-pressure Hg arc lamp (Exfo Acticure 4000) using 365 nm light with a standard intensity of 2.3  $\text{mW}/\text{cm}^2$  (unless otherwise noted). Spectra were collected every 0.2 s at 8  $\text{cm}^{-1}$  resolution during the course of polymerization. The percent double bond conversion was calculated from peak height changes associated with polymerization, as reported elsewhere.<sup>35</sup> Thiol monomer conversion was monitored at the S–H stretching peak at 2569  $\text{cm}^{-1}$  while ene monomer conversion was monitored at the =C–H stretching peak around 3078  $\text{cm}^{-1}$ . Polymerization rates ( $\text{s}^{-1}$ ) for both thiol and ene were determined from the time derivative of RTIR conversion profiles.

In addition to examining polymer evolution, RTIR is useful in examining LC phase separation and order in polymer/LC systems.<sup>12,13,35</sup> The extent of the decrease in cyano absorbance from the value before polymerization is indicative of the amount of LC in the nematic phase in the formed PDLC. The thermotropic nature of BL037 was utilized to determine the absolute absorbance change of this LC in its isotropic state vs its nematic state. On a unit scale, the absorbance of bulk BL037 at 2225  $\text{cm}^{-1}$  in the isotropic phase is 1.0 and 0.78 in the nematic phase. Before polymerization of PDLCs, BL037 is isotropic as the formulation is homogeneously mixed. Upon phase separation of BL037, the LC undergoes an isotropic-to-nematic transition. The ratio of the absorbance change at 2225  $\text{cm}^{-1}$  during the polymerization of PDLCs to the absolute absorbance change of the neat LC was used to calculate the fraction of LC in the nematic phase (nematic fraction) as given in eq 1:

$$\text{nematic fraction} = \frac{A_0 - A_t}{0.22} \quad (1)$$

where  $A_0$  is the average absorbance (unit scale) at 2225  $\text{cm}^{-1}$  for the 10 s before polymerization and  $A_t$  is the absorbance (unit scale) at time  $t$  during polymerization. In a given PDLC, if all the BL037 phase separates into droplets exhibiting the nematic phase, the relative absorbance at 2225  $\text{cm}^{-1}$  should decrease by 22%. To further examine the influence of formulation changes on phase separation kinetics in PDLCs, the rate of nematic appearance was determined from the time derivative of normalized cyano peak height data.

A scanning electron microscope (SEM, Hitachi S-9000, 5 keV) was used to directly examine polymer/LC morphology. PDLC formulations with 175  $\mu\text{m}$  glass spacers were polymerized between glass microscope slides via the RTIR light source at 2.3  $\text{mW}/\text{cm}^2$ , subjected to methanol extraction, air-dried, and freeze-fractured with liquid nitrogen. Samples were mounted on aluminum stubs via black carbon tape to enable analysis of the bulk morphology. After samples were mounted, a 2–5 nm coat of tungsten was applied by a sputter coater (Emiteon K550).

Electrooptic behavior of fabricated PDLCs was examined using an optical setup previously reported.<sup>33</sup> PDLCs were polymerized between indium–tin oxide (ITO) glass slides with 15  $\mu\text{m}$  glass spacers. The transmission of light through the PDLC was examined with a spectrometer (Ocean Optics) as voltage was increased stepwise (square wave, 1 kHz, 5 V rms) until the PDLC became transparent.

## Results and Discussion

Simultaneously examining both polymer evolution and liquid crystal (LC) phase separation during the formation of polymer dispersed liquid crystals (PDLCs) has been instrumental in

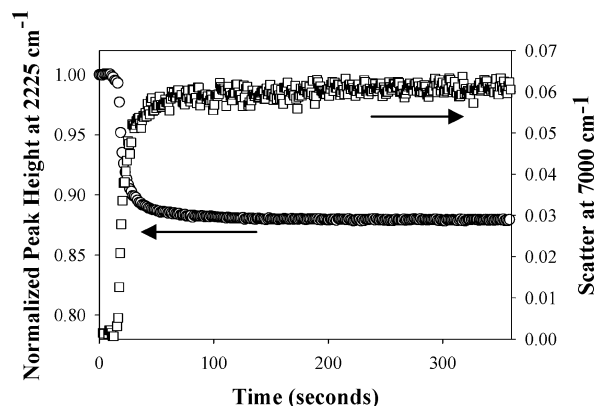


**Figure 2.** RTIR examination of LC phase separation in polymerization of trithiol/diene at 1  $\text{mW}/\text{cm}^2$ . Both normalized cyano peak height at 2225  $\text{cm}^{-1}$  (O) and scatter at 7000  $\text{cm}^{-1}$  (□) are measured as a function of time.

understanding which factors during polymerization are critical to dictating LC phase separation and, ultimately, polymer/LC morphology. In the early efforts by Kloosterboer et al., a photodifferential scanning calorimeter (DSC) was combined with a turbidity accessory to access information regarding the role that variables such as light intensity (polymerization rate), cross-link density, and the chemical makeup of LC play on the polymer-induced phase separation process.<sup>8–10</sup> More recently, real-time infrared (RTIR) has been used to simultaneously examine LC phase separation and nematic order in PDLCs made from NOA65 and the cyanobiphenyl liquid crystal E7.<sup>12,13</sup> During the polymerization of PDLCs, the initially clear mixture becomes turbid upon polymer-induced phase separation of the LC. With LC phase separation, the LC molecules transition from isotropic to nematic. Both these phenomena impart changes to the IR spectra that when monitored in real time serve as a means to study LC phase separation as a function of the polymerization.

The changes in IR peak height at 2225  $\text{cm}^{-1}$  and scatter at 7000  $\text{cm}^{-1}$  are shown in Figure 2 for the polymerization of a trithiol/diene-based PDLC at 1  $\text{mW}/\text{cm}^2$ . The polymerization, initiated after 10 s of data collection, exhibits a short lag before the peak height at 2225  $\text{cm}^{-1}$  decreases and the scatter at 7000  $\text{cm}^{-1}$  increases. The decrease in peak height at 2225  $\text{cm}^{-1}$  is associated with the increasing appearance of the nematic phase as LC phase separates. The decreased transmission at 7000  $\text{cm}^{-1}$  occurs as the polymer/LC morphology forms with droplets large enough to scatter light at this wavelength (1.4  $\mu\text{m}$ ). While Bhargava<sup>12,13</sup> has shown minor differences in the onset of nematic ordering and scattering, it appears that they are quite similar under the conditions of this study.<sup>38</sup> Unfortunately, scatter during the formation of PDLCs is droplet size dependent and therefore not relevant in comparing LC phase separation with PDLC formulations of dramatically different polymer/LC morphology. For example, PDLCs made from trithiol/divinyl ether exhibit LC droplets as small as 300 nm and impart no scatter at 7000  $\text{cm}^{-1}$ . Therefore, this work will exclusively utilize the examination of the isotropic to nematic transition at 2225  $\text{cm}^{-1}$  as a measure of LC phase separation.

Most reports of PDLCs have utilized either acrylate or thiol–ene polymer as host. The significant differences in the polymerization mechanism, polymerization kinetics, and polymer gel point of acrylate and thiol–ene systems distinguish the polymer-induced phase separation process in these systems. To contrast polymer-induced phase separation in PDLCs based on acrylate and thiol–ene polymerization, Figure 3a shows RTIR examination of LC phase separation (as monitored by the appearance

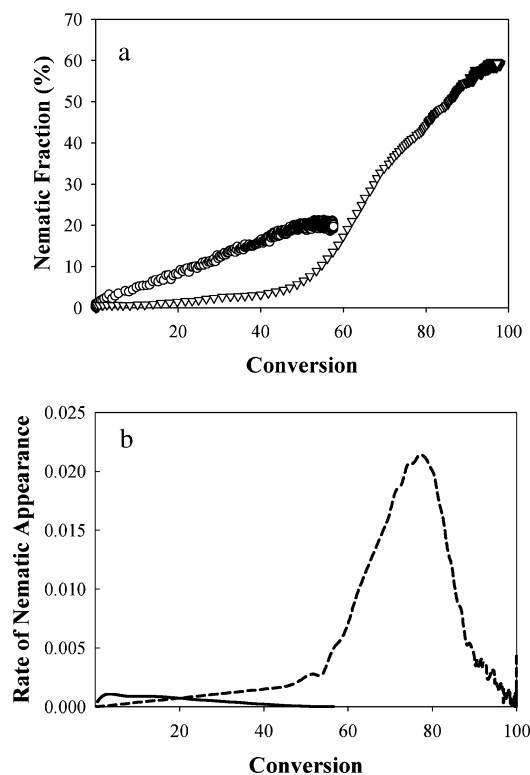


**Figure 3.** (a) Nematic fraction (%) vs monomer conversion for acrylate-based PDLC (O) and trithiol/diene PDLC ( $\nabla$ ). (b) Rate of nematic appearance vs monomer conversion for acrylate-based PDLC (—) and trithiol/diene PDLC (- - -). Polymerization initiated with 1 mW/cm<sup>2</sup>.

of nematic order) as a function of double bond conversion for pentaacrylate-based PDLCs. The evolution of the nematic fraction (i.e., the fraction of LC molecules in the nematic mesophase) in the PDLCs is plotted against monomer conversion in Figure 3a. In the pentaacrylate-based PDLC, the appearance of the nematic phase is immediate and steadily increases over the range of double bond conversion until the ultimate conversion of 55% is reached. The evolution of the nematic phase is much different for the trithiol/diene PDLC formulation. Minor increases in nematic fraction are observed until 50% thiol conversion, followed by a rapid increase that allows ~60% of the nematic phase to appear. About two-thirds of LC phase separation in this trithiol/diene PDLC occurs between 50 and 70% thiol conversion.

It is clear from Figure 3a that the polymerization mechanism is very influential on the evolution and extent of LC phase separation. The phase separation kinetics are more clearly shown in Figure 3b, where the rate of nematic appearance is plotted against conversion for the acrylate- and thiol–ene-based PDLCs. The rate of nematic appearance is the time derivative of the normalized cyano peak height data and indicates the rate at which the LC is transitioning from isotropic to nematic. The rate of nematic appearance for the acrylate-based PDLC rises to a maximum at less than 3% double bond conversion and thereafter tapers off to zero over the range of acrylate double bond conversion. In contrast, the rate of nematic appearance for the trithiol/diene PDLC rises steadily until ~50% thiol conversion and then sharply increases to a maximum at around 75% thiol conversion. The overall maximum rate of nematic appearance is nearly 10 times greater for the thiol–ene PDLC than the acrylate-based PDLC.

These results regarding the appearance of the nematic phase give significant information regarding phase separation as well.

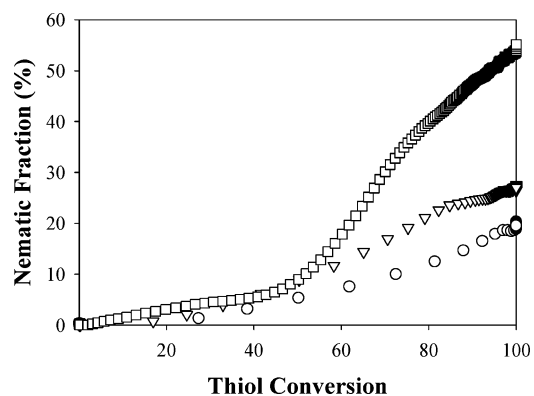


**Figure 4.** Nematic fraction (%) vs thiol monomer conversion for trithiol/diene PDLC polymerized at 2.3 ( $\square$ ), 23 ( $\nabla$ ), and 46 mW/cm<sup>2</sup> (O).

From Figure 3a it is evident that thiol–ene PDLCs exhibit a much higher percentage of nematic LC and thus higher degree of LC phase separation than the acrylate-based PDLC. Furthermore, from Figure 3b, the conversion at which the maximum rate of nematic appearance occurs shifts from less than 3% in acrylate-based PDLCs to upward of 75% in the thiol–ene PDLC. Interestingly, the maximum rate of nematic appearance occurs nearly exactly at the gel point for both PDLC systems. The differences in nematic fraction and rate of nematic appearance as well as their dependence on conversion are directly related to differences in polymerization mechanism and how they affect the gel point. Since the gel point of this acrylate system is reached almost immediately after polymerization, LC phase separation primarily occurs via liquid–gel demixing; i.e., the LC is phase separating from a gelled polymer. For the trithiol/diene PDLC, the theoretical gel point is calculated to occur at 71% conversion. Therefore, up to 71% conversion, demixing in this thiol–ene mixture occurs mostly through liquid–liquid demixing; i.e., the LC is phase separating from a liquid solution. After the gel point at 71% conversion, phase separation continues via liquid–gel demixing albeit at a reduced rate. Of the two demixing processes (liquid–liquid and liquid–gel) it seems that liquid–liquid occurs at a faster rate and results in greater LC phase separation in PDLCs. The unique behavior of LC demixing occurring between 50 and 71% conversion in thiol–ene systems may indicate that the solubility of the LC is reduced as the molecular weight of the liquid matrix increases, causing greater liquid–liquid demixing.

The polymerization kinetics of thiol–ene and acrylate systems are very different and may be the source for some of the reduction of LC phase separation in acrylate PDLCs. To examine more clearly the influence of polymerization kinetics on PDLC formation, the trithiol/diene PDLC was studied over a range of light intensities. Previous work has shown that increasing the polymerization rate by increasing light intensity results in reduced LC droplet size in PDLCs.<sup>14,39</sup> RTIR examination of nematic fraction and double bond conversion for the trithiol/diene based thiol–ene PDLC over a range of light intensities is shown in Figure 4 and echoes these previous results. Increasing light intensity from 2.3 to 46 mW/cm<sup>2</sup> increases polymerization rate, significantly reducing the ultimate nematic fraction from 50% to 20%. In examining the evolution of the nematic fraction, the liquid–liquid demixing process up to 50% thiol conversion is very similar despite the change in light intensity. After 50% thiol conversion, the evolution of LC phase separation (as indicated by the appearance of the nematic phase) for the three light intensities significantly diverges. The theoretical gel point for trithiol/diene PDLC is 71% thiol

conversion, which is independent of light intensity. As previously discussed in Figure 3, LC phase separation from 0 to 71% conversion in trithiol/diene PDLCs occurs via liquid–liquid demixing. The unique behavior between 50 and 71% conversion evident in both Figure 3 and 4 is likely due to reduced monomer concentration and increased molecular weight in the reaction medium. These changes reduce the solubility of the LC, which in turn increases the rate of liquid–liquid demixing. As a thermodynamic phenomenon, LC phase separation is a time-dependent process. Increasing the light intensity increases the polymerization rate, which will reduce the amount of time between 50 and 71% conversion. Reducing the amount of time for LC phase separation to occur by liquid–liquid demixing between 50 and 71% conversion thereby limits the extent of LC phase separation.

Figures 3 and 4 show that LC phase separation in PDLCs strongly depends on the gel point and polymerization kinetics. As previous research of bulk thiol–ene polymerization has shown, thiol and ene monomers of various functionality and electron density are available that polymerize at dramatically different rates and form cross-linked polymers with gel point conversions that range from 33 to 86%. A first step toward tailoring thiol–ene PDLC formulations is determining the influence, if any, that thiol–ene stoichiometry plays in the formation of PDLCs. To this end, the polymerization kinetics and nematic fraction of thiol–ene PDLC formulations of 1:1 (stoichiometric), 1:1.33 (excess ene), and 1:0.66 (excess thiol) trithiol to diene PDLC formulations are shown in Figure 5a–c. As shown in Table 1, varying the stoichiometric ratios of trithiol and diene shifts the gel point from 71% in a stoichiometric mixture of trithiol/diene to 81% (1:1.33 trithiol to diene) and 86% (1:0.66 trithiol to diene) in nonstoichiometric formulations.<sup>36</sup>

To determine whether thiol–ene stoichiometry is influential on polymerization kinetics in PDLCs, RTIR determination of the ene polymerization rate for 1:1, 1:1.33, and 1:0.66 trithiol to diene PDLC formulations is shown in Figure 5a. Figure 5a is a plot of the rate of ene conversion vs the conversion of ene monomer. As the concentration of thiol functional groups increases, the polymerization rate increases. The PDLC containing excess thiol monomer has a polymerization rate 60% greater than the stoichiometric mixture of trithiol and diene. The presence of excess ene in the 1:1.33 trithiol to diene mixture reduces polymerization rate dramatically.

In addition to influencing polymerization rate, thiol–ene stoichiometry also impacts the overall conversion of the system. Figure 5b plots thiol conversion vs ene conversion for 1:1, 1:1.33, and 1:0.66 trithiol to diene PDLC formulations. Because of the step-growth polymerization mechanism, the plot of thiol conversion vs ene conversion is linear. In the stoichiometric mixture, both thiol and ene monomer achieve 100% conversion. In the sample containing excess thiol monomer, ene monomer goes to 100% conversion while thiol monomer achieves ~60% conversion. In the sample containing excess ene monomer, thiol monomer goes to 100% conversion while ene monomer achieves ~65% conversion. Therefore, the influence of thiol–ene stoichiometry is not limited to kinetics, but the impact of unreacted functional groups on polymer network structure must also be considered.

Changing the stoichiometric ratio of trithiol and diene shifts the polymer gel point (Table 1), polymerization rate (Figure 5a), and overall conversion of thiol and ene monomer (Figure 5b). The influence of thiol–ene stoichiometry on structure development of thiol–ene PDLC systems may also influence

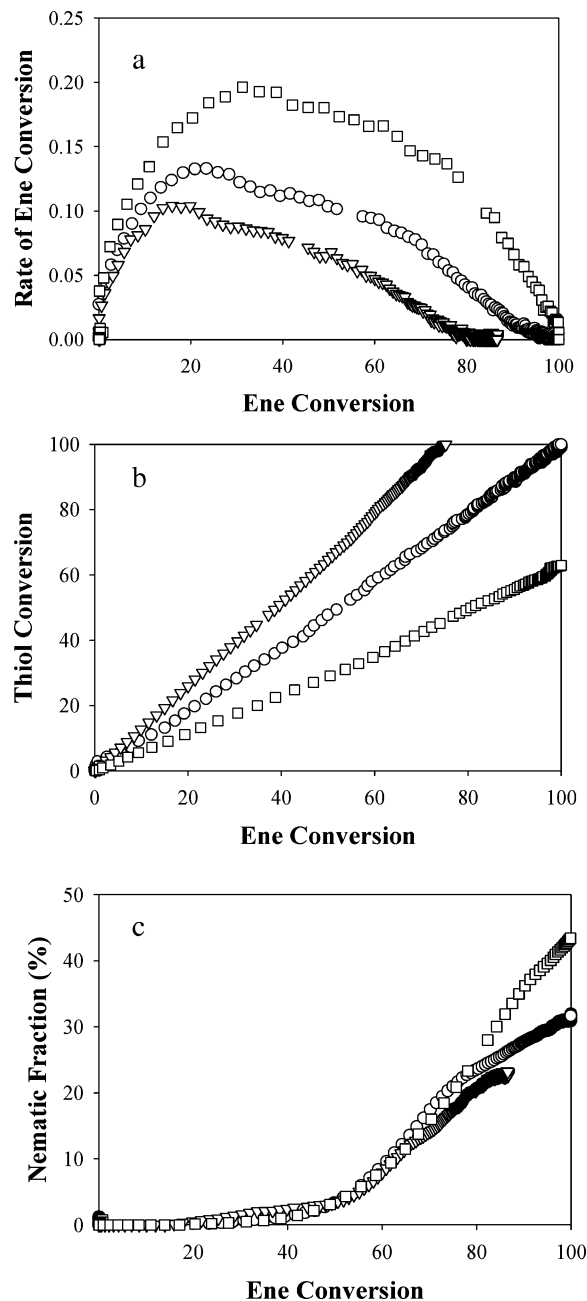


**Figure 5.** (a) Rate of thiol conversion vs thiol conversion, (b) rate of ene conversion vs ene conversion, and (c) nematic fraction (%) vs ene conversion for trithiol/diene PDLCs of various stoichiometry: 1:0.66 trithiol to diene (excess thiol) ( $\square$ ), 1:1 trithiol to diene (stoichiometric) ( $\circ$ ), and 1:1.33 trithiol to diene (excess ene) ( $\nabla$ ). Polymerization initiated with 17 mW/cm<sup>2</sup>.

LC phase separation. To determine whether thiol–ene stoichiometry has any influence on phase separation, Figure 5c compares the nematic fraction vs ene conversion for trithiol/diene PDLCs with different stoichiometric ratios. The maximum percentage of nematic fraction increases dramatically with thiol concentration from 25% (1:1.33) to 45% (1:0.66). Interestingly, the sample containing excess thiol (1:0.66) has greater LC phase separation than the PDLC formulation containing a stoichiometric mixture of trithiol and diene. One possible explanation for the increase in nematic fraction in the PDLC containing 1:0.66 trithiol to diene may be associated with decreased LC solubility due to reduced ene concentration. In addition to the reduced solubility of LC in polymerizations containing excess thiol, the influence of thiol–ene stoichiometry on gel point may also be a factor. From Figure 5c, the evolution of the nematic

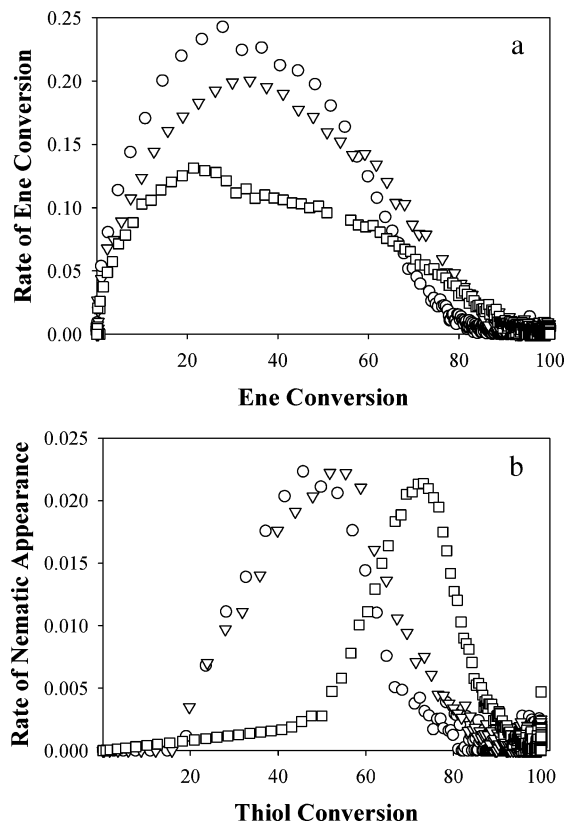


**Figure 6.** (a) Rate of ene conversion vs ene conversion and (b) rate of nematic appearance vs thiol conversion for thiol–ene PDLCs with trithiol/tetraene (O), trithiol/triene (∇), and trithiol/diene (□).

phase for the polymerization of the stoichiometric, excess thiol, and excess ene PDLCs is virtually identical until  $\sim 65\%$  ene conversion. Notably, 65% ene conversion is the gel point conversion (equivalent to 86% thiol conversion) of the 1:1.33 trithiol to diene formulation. At  $\sim 70\%$  ene conversion, the nematic fraction of the stoichiometric PDLC also diverges from the 1:0.66 trithiol/diene PDLC. The stoichiometric PDLC has a gel point of 71% conversion. The consistency in liquid–liquid demixing in the three trithiol/diene formulations until gelation seems to indicate that the gel point is a critical factor in enabling greater LC phase separation, perhaps even more important than polymerization kinetics.

The polymer gel point in thiol–ene polymerization can also be shifted by changing monomer functionality. The influence of ene monomer functionality on the polymerization kinetics and LC phase separation is examined in Figure 6a,b. Figure 6a plots ene conversion rate vs ene conversion for thiol–ene PDLC formulations containing trithiol polymerized with allyl ether monomers of functionality two to four. All formulations were stoichiometrically matched, resulting in nearly complete conversion of thiol and ene. Increasing ene monomer functionality significantly increases the polymerization rate. The polymerization rate of trithiol/tetraene PDLC is almost double the trithiol/diene PDLC. The rate of polymerization of thiol–allyl ether systems, as shown elsewhere, is first order with regard to thiol group concentration and zero order with regard to double bond concentration.<sup>40,41</sup> As the functionality of the ene monomer increases, the monomer molecular weight per functional group decreases. Therefore, the concentration of thiol functional groups in stoichiometric mixtures containing 1 mol of diene, triene, and tetraene increases from 0.67, 1.0, and 1.33 as ene monomer functionality increases. The increase in thiol concentration with increasing ene monomer functionality increases the polymeri-

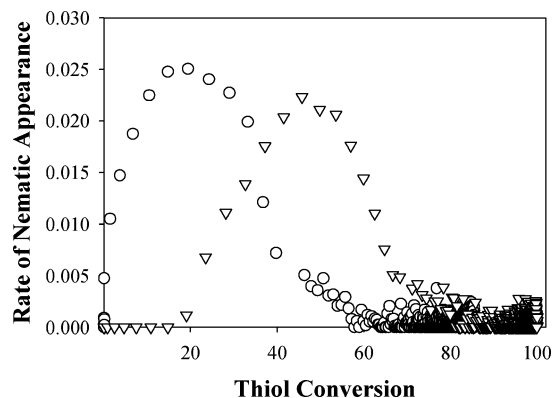


**Figure 7.** Rate of nematic appearance vs ene conversion for thiol–ene PDLCs with tetrathiol/tetraene (O) and trithiol/tetraene (∇).

**Table 2. Maximum Nematic Fraction (%) for Thiol–Ene PDLCs**

name	nematic fraction (%)
trithiol/diene	55
trithiol/triene	29
trithiol/tetraene	20
tetrathiol/tetraene	16

zation rate of thiol–ene PDLCs.

Increasing ene monomer functionality shifts the gel point to lower conversion while also increasing polymerization rate. Such changes in polymerization kinetics and gelation should have significant influence in LC phase separation. For examination of phase separation as a function of monomer functionality, the rate of nematic appearance is plotted against thiol conversion in Figure 6b for the three PDLC mixtures based on diene, triene, and tetraene. The rate of nematic appearance, the time derivative of the normalized cyano peak height data, clearly illustrates the influence of polymer gel point on phase separation kinetics. With respect to thiol conversion, all three PDLC mixtures exhibit similar initial rates of nematic appearance, indicating similar liquid–liquid demixing up to  $\sim 15\%$  thiol conversion. At this point in the polymerization, both the PDLC made with the triene and the tetraene exhibit a rapid increase in the rate of nematic appearance. The PDLC mixture with the diene continues a steady increase in rate up to 50% thiol conversion until it also exhibits a similar rapid rate increase. In all three PDLC formulations, the maximum in the rate of nematic appearance is near the gel point of the respective system (Table 1).

Similar results are seen in examining thiol monomer functionality. The rate of nematic appearance is plotted against thiol conversion in Figure 7 for trithiol/tetraene and tetrathiol/tetraene PDLC formulations. Increasing thiol monomer functionality in PDLCs shifts the maximum in the rate of nematic appearance from 45% thiol conversion in trithiol/tetraene to around 20% thiol conversion in tetrathiol/tetraene. Increasing thiol functionality from three to four shifts the theoretical polymer gel point from 41% to 33% conversion. As expected, this change in polymer gel point again influences the evolution of LC phase separation. Thiol monomer functionality has little, if any, influence on polymerization rate in PDLCs. Unlike ene monomer functionality, increasing thiol monomer functionality maintains the monomer molecular weight to functionality ratio. Since the thiol functional group concentration is the same in PDLCs based on trithiol and tetrathiol, the polymerization rate of these two systems is equivalent.

In addition to influencing the polymer gel point and the LC demixing process, monomer functionality also limits the LC nematic fraction. Shown in Table 2 is the nematic fraction for the thiol–ene PDLC mixtures examined in Figures 6 and 7. As

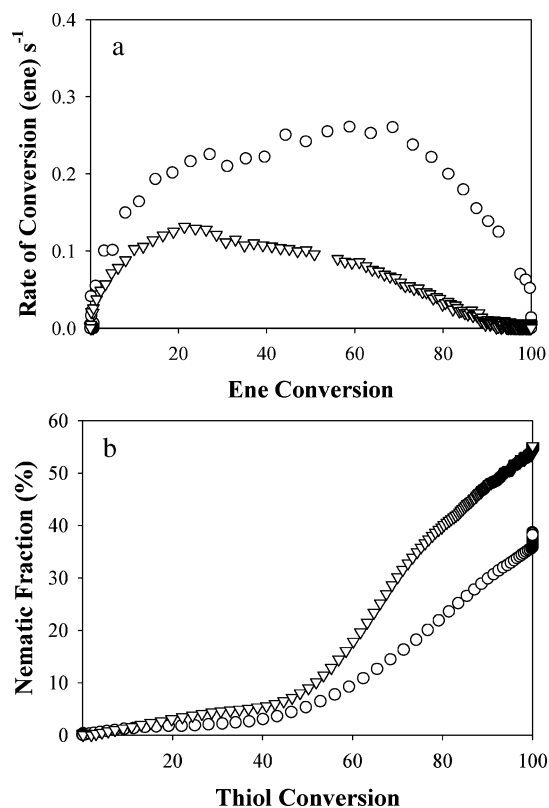


**Figure 8.** (a) Rate of ene conversion vs ene conversion and (b) nematic fraction vs thiol conversion for PDLCs with trithiol/divinyl ether (O) and trithiol/diene ( $\nabla$ ).

ene monomer functionality increases from two to four in polymerization with trithiol, the maximum nematic fraction markedly decreases from 55% (trithiol/diene) to 20% (trithiol/tetraene). Similarly, as thiol monomer functionality is increased from three to four in polymerization with the tetraene, the extent of nematic fraction decreases from 20% to 16%. For both thiol and ene monomer functionality, gel points at higher conversion leads to increased LC phase separation. Ene monomer functionality, with its significant influence on polymerization rate, serves to further limit the amount of nematic LC and is therefore

more influential than thiol monomer functionality in dictating the extent of LC phase separation in thiol–ene PDLCs.

As documented by Morgan in 1977,<sup>28</sup> thiol–ene polymerization rates are highly dependent on the structure of the ene monomer. While thiol–allyl ether polymerization is relatively fast, thiol–vinyl ether polymerization is known to polymerize at an even faster rate. Thiol–ene-based PDLCs containing electron-rich ene monomers including divinyl ethers have been previously examined.<sup>42</sup> The polymerization kinetics of PDLC made from trithiol/divinyl ether are compared to the trithiol/diene PDLC formulation in Figure 8a. As expected, the rate of the trithiol/divinyl ether PDLC formulation is double that observed in the diene. The only difference between the thiol–ene polymerization of divinyl ether and diene are the kinetics, as these polymerizations should have identical gel points.

The influence of trithiol/divinyl ether PDLC on nematic fraction is examined in Figure 8b, once again in comparison to trithiol/diene. As expected, the increased polymerization rate in trithiol/divinyl ether based PDLC reduces ultimate nematic fraction relative to trithiol/diene. The trithiol/divinyl ether and trithiol/diene PDLC have similar evolution of the nematic phase up to  $\sim 50\%$  thiol conversion when the increased polymerization rate in trithiol/divinyl ether limits liquid–liquid demixing, similar to the influence of increased light intensity described previously.

Changing the extent of LC phase separation and/or polymerization rate of thiol–ene PDLCs is known to dramatically influence LC droplet size, a critical factor in determining PDLC performance. To this end, the morphology of the thiol–ene PDLCs studied here was examined with scanning electron microscopy (SEM). As shown in Figure 9a–f, the PDLCs all exhibit droplet morphology regardless of polymer composition. In comparing the morphology of trithiol/diene in Figure 9a to tetrathiol/diene in Figure 9d, reducing thiol monomer functionality decreases LC droplet size from around  $1 \mu\text{m}$  to nearly  $800 \text{ nm}$ . Similarly, the comparisons of trithiol/diene (Figure 9a) to trithiol/triene (Figure 9b) and trithiol/tetraene (Figure 9c) show that increasing ene monomer functionality also decreases LC droplet size, to as low as  $400 \text{ nm}$  (trithiol/tetraene). Since thiol monomer functionality is not influential on the polymerization

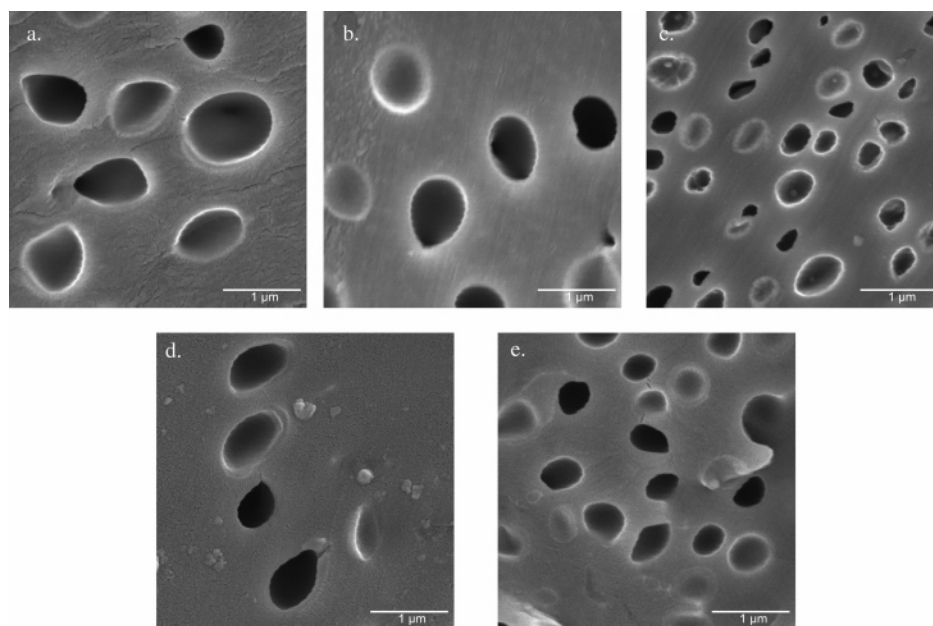


**Figure 9.** Morphology of PDLCs as a function of monomer functionality and ene monomer electron density: (a) trithiol/diene, (b) trithiol/triene, (c) trithiol/tetraene, (d) tetrathiol/diene, and (e) trithiol/divinyl ether.

**Table 3. Electrooptic Switching Behavior of Thiol–Ene-Based PDLCs**

PDLC formulation	average LC droplet size	switching field (V/ $\mu\text{m}$ )
trithiol/diene	1 $\mu\text{m}$	5.1
trithiol/tetraene	400 nm	7.7
NOA65	400 nm	7.6

rate in the PDLC formulations examined, the reduced LC droplet size is related to the changed in gel point. As shown in Figure 7, increasing thiol monomer functionality shifts the onset of liquid–gel demixing, limiting LC phase separation. Subsequently, the LC droplets have less time to grow and coalesce, reducing LC droplet size. Similarly, the LC droplet size reduction with increasing ene monomer functionality is correlated to the polymer gel point. Additionally, ene monomer functionality also shows a marked effect on polymerization rate, further reducing LC droplet size in PDLCs made with higher functionality ene monomer.

PDLCs containing trithiol/divinyl ether (Figure 9e) show reduced LC droplet size in comparison to trithiol/diene (Figure 9a) with an identical gel points. Increasing the polymerization kinetics by incorporating divinyl ether reduces LC droplet size from around 1  $\mu\text{m}$  in the trithiol/diene PDLC (Figure 9a) to nearly 300 nm. The reduction in LC droplet size associated with the kinetic influence of divinyl ether corroborate previous results demonstrating the influence of light intensity on NOA65-based PDLC droplet size.<sup>14,39</sup>

To illustrate the role of changes to polymer/LC morphology on electrooptic switching behavior, the switching voltage of the trithiol/tetraene and trithiol/diene PDLCs was determined and compared to a PDLC based on NOA65, as shown in Table 3. Switching voltage is known to be a function of the size and aspect ratio of the LC droplets.<sup>2</sup> Morphology examination, shown in Figure 8, indicates that the aspect ratio of the LC droplets in the various PDLCs are nearly identical, meaning that the determining factor in switching will be the LC droplet size. The switching fields for the PDLCs examined in Table 3 are as expected, directly correlated to LC droplet size. Increasing ene monomer functionality from two to four serves to increase switching field from 5.1 to 7.7 V/ $\mu\text{m}$ , due to the corresponding LC droplet size reduction associated with the trithiol/tetraene formulation. Comparatively, this trithiol/tetraene PDLC formulation has similar switching behavior as NOA65, which requires a field of 7.6 V/ $\mu\text{m}$ .

## Conclusion

The polymerization kinetics, LC phase separation, and morphology of PDLC formulations formed in thiol–ene systems with different light intensity, stoichiometry, and functionality were examined. Interestingly, both polymerization kinetics and gel point significantly influence the LC phase separation process. Examination of LC phase separation of trithiol/diene PDLCs over a range of light intensities shows that increased polymerization rate limits LC phase separation. The influence of polymer gel point is evident in comparing thiol–ene and acrylate-based PDLCs and when varying thiol and ene monomer functionality. The high gel point conversion inherent in thiol–ene polymers allow LC phase separation to proceed primarily via liquid–liquid demixing rather than the liquid–gel demixing process seen in acrylate systems. In thiol–ene PDLCs, increasing monomer functionality shifts the gel point to lower monomer conversion, subsequently limiting the amount of LC phase separation. Decreases in polymer gel point trigger the transition in LC phase separation from liquid–liquid to liquid–gel

demixing. Allowing LC phase separation to proceed via liquid–liquid demixing into high monomer conversion enables greater LC phase separation. Thiol–ene stoichiometry in PDLC formulations is also influential on polymerization and phase separation as PDLCs containing excess thiol monomer have faster polymerization rate and greater LC phase separation. Comparison of allyl ether thiol–ene PDLCs to fast-reacting systems containing divinyl ether further illustrates the influence of polymerization kinetics on LC phase separation and LC droplet size. PDLCs based on divinyl ether have reduced LC phase separation and reduced LC droplet size, and thereby improvement in electrooptic properties, in comparison to difunctional allyl ether systems.

**Acknowledgment.** Support of this work by the Air Force Research Labs Materials and Manufacturing Directorate is gratefully acknowledged.

## References and Notes

- Mucha, M. *Prog. Polym. Sci.* **2003**, *28*, 837.
- Drzaic, P. *Liquid Crystal Dispersions*; World Scientific Publishing: Singapore, 1995; Vol. 1.
- Higgins, D. A. *Adv. Mater.* **2000**, *12*, 251.
- Doane, J. W.; Vaz, N. A.; Wu, B. G.; Zumer, S. *Appl. Phys. Lett.* **1986**, *48*, 269.
- Ono, H.; Shimokawa, H.; Emoto, A.; Kawatsuki, N. *Polymer* **2003**, *44*, 7971.
- LeGrange, J. D.; Carter, S. A.; Fuentes, M.; Boo, J.; Freeny, A. E.; Cleveland, W.; Miller, T. M. *J. Appl. Phys.* **1997**, *81*, 5984.
- Grand, C.; Achard, M. F.; Hardouin, F. *Liq. Cryst.* **1997**, *22*, 287.
- Boots, H. M. J.; Kloosterboer, J. G.; Serbutoviez, C.; Touwslager, F. *J. Macromolecules* **1996**, *29*, 7683.
- Kloosterboer, J. G.; Serbutoviez, C.; Touwslager, F. *J. Polymer* **1996**, *37*, 5937.
- Serbutoviez, C.; Kloosterboer, J. G.; Boots, H. M. J.; Touwslager, F. *J. Macromolecules* **1996**, *29*, 7690.
- Fouassier, J.-P. *Photoinitiation, Photopolymerization and Photocuring: Fundamentals and Applications*; Hanser/Gardner: Cincinnati, 1995.
- Bhargava, R.; Wang, S. Q.; Koenig, J. L. *Macromolecules* **1999**, *32*, 8982.
- Bhargava, R.; Wang, S. Q.; Koenig, J. L. *Macromolecules* **1999**, *32*, 8989.
- Lovinger, A. J.; Amundson, K. R.; Davis, D. D. *Chem. Mater.* **1994**, *6*, 1726.
- Smith, G. W. *Phys. Rev. Lett.* **1993**, *70*, 198.
- Smith, G. W. *Mol. Cryst. Liq. Cryst.* **1994**, *239*, 63.
- Smith, G. W. *Mol. Cryst. Liq. Cryst.* **1994**, *241*, 77.
- Vaz, N. A.; Smith, G. W.; Montgomery, G. P., Jr. *Liq. Cryst.* **1987**, *146*, 1.
- Senyurt, A. F.; Warren, G.; Whitehead, J. B.; Hoyle, C. E. *Polymer* **2006**, *47*, 2741.
- Leclercq, L.; Maschke, U.; Ewen, B.; Coqueret, X.; Mechernene, L.; Benmouna, M. *Liq. Cryst.* **1999**, *26*, 415.
- Vaia, R. A.; Tomlin, D. W.; Schulte, M. D.; Bunning, T. J. *Polymer* **2001**, *42*, 1055.
- Roussel, F.; Buisine, J.-M.; Maschke, U.; Coqueret, X. *Liq. Cryst.* **1998**, *24*, 555.
- Vaz, N. A.; Smith, G. W.; Montgomery, G. P., Jr. *Mol. Cryst. Liq. Cryst.* **1987**, *146*, 17.
- Doane, J. W.; Chidichimo, G.; Vaz, N. A. U.S. Patent No. 4 688 900, 1987.
- Simoni, F.; Cipparrone, G.; Umeton, C.; Arabia, G.; Chidichimo, G. *Appl. Phys. Lett.* **1989**, *54*, 896.
- Schulte, M. D.; Clarson, S. J.; Natarajan, L. V.; Tomlin, D. W.; Bunning, T. J. *Liq. Cryst.* **2000**, *27*, 467.
- Carlsson, I.; Harden, A.; Lundmark, S.; Manea, A.; Rehnberg, N.; Svensson, L. In *ACS Symposium Series 847*; Belfield, K. D., Crivello, J. V., Eds.; American Chemical Society: Washington, DC, 2003.
- Morgan, C. R.; Magnotta, F.; Ketley, A. D. *J. Polym. Sci., Part A: Polym. Chem.* **1977**, *15*, 627.
- Chiou, B.-S.; English, R. J.; Khan, S. A. *Macromolecules* **1996**, *29*, 5368.
- Chiou, B.-S.; Khan, S. A. *Macromolecules* **1997**, *30*, 7322.
- Hoyle, C. E.; Lee, T. Y.; Roper, T. *J. Polym. Sci., Part A: Polym. Chem.* **2004**, *42*, 5301.
- Jacobine, A. F. *Radiat. Curing Polym. Sci. Technol.* **1993**, *3*, 219.



- (33) Natarajan, L. V.; Shepherd, C. K.; Brandelik, D. M.; Sutherland, R. L.; Chandra, S.; Tondiglia, V. P.; Tomlin, D.; Bunning, T. J. *Chem. Mater.* **2003**, *15*, 2477.
- (34) White, T. J.; Natarajan, L. V.; Tondiglia, V. P.; Lloyd, P. F.; Bunning, T. J.; Guymon, C. A. *Macromolecules*, in press.
- (35) White, T. J.; Liechty, W. B.; Natarajan, L. V.; Tondiglia, V. P.; Bunning, T. J.; Guymon, C. A. *Polymer* **2006**, *47*, 2289.
- (36) Odian, G. *Principles of Polymerization*, 4th ed.; John Wiley and Sons: New York, 2004.
- (37) Lovell, L. G.; Berchtold, K. A.; Elliott, J. E.; Lu, H.; Bowman, C. N. *Polym. Adv. Technol.* **2001**, *12*, 335.
- (38) The polymerization kinetics in this report are much faster due to the usage of 1 wt % DC-4265. It should also be noted that the LC BL037, while similar to E7, exhibits lower solubility limits in thiol-ene mixtures.
- (39) Carter, S. A.; LeGrange, J. D.; White, W.; Boo, J.; Wiltzius, P. *J. Appl. Phys.* **1997**, *81*, 5992.
- (40) Cramer, N. B.; Davies, T.; O'Brien, A. K.; Bowman, C. N. *Macromolecules* **2003**, *36*, 4631.
- (41) Cramer, N. B.; Reddy, S. K.; O'Brien, A. K.; Bowman, C. N. *Macromolecules* **2003**, *36*, 7964.
- (42) Jacobine, A. F.; Woods, J. G.; Rakas, M. A. WO 9425508, US, 1994.

MA061828U